Supplementary Information

for

An amphiphilic material arginine-arginine-bile acid promotes α-synuclein amyloid formation

Yuxi Lin[1,†], So-Hyeon Park[2,3†], Eugene Bok[4], Yunseok Heo[1], Seong-Bin Yang[3], Yoon-Sun Yi[5], Jun-Hyuck Lee[2,3], Donghyun Seo[1,6], Eunae Jo[1], Sungsu Lim[7], Yun Kyung Kim[7,8], József Kardos[9], Kyoung-Seok Ryu[1,10], Jaekwang Kim[4], Jooho Park[2,3,*], and Young-Ho Lee[1,10,11,*]

[1]Research Center for Bioconvergence Analysis, Korea Basic Science Institute (KBSI), Chungbuk 28119, Republic of Korea

[2]Department of Biomedical Chemistry, College of Biomedical & Health Science, Konkuk University, Chungju 27478, Republic of Korea

[3]Department of Applied Life Sciences, Graduate School, BK21 Program, Konkuk University, Chungju 27478, Republic of Korea

[4]Dementia Research Group, Korea Brain Research Institute (KBRI), Daegu 41062, Republic of Korea

[5]Electron Microscopy & Spectroscopy Team, Korea Basic Science Institute (KBSI), Chungbuk 28119, Republic of Korea

[6]Department of Proteome Structural Biology, University of Science and Technology (UST), Daejeon 34113, Republic of Korea

[7]Brain Science Institute, Korea Institute of Science and Technology (KIST), Seoul 02792, Republic of Korea

[8]Division of Bio-Medical Science & Technology, KIST School, University of Science and Technology (UST), Seoul 02792, Republic of Korea

[9]Department of Biochemistry, Institute of Biology, ELTE Eötvös Loránd University, H-1117 Budapest, Hungary

[10]Bio-Analytical Science, University of Science and Technology (UST), Daejeon 34113, Republic of Korea

[11]Graduate School of Analytical Science and Technology (GRAST), Chungnam National

University, Daejeon 34134, Republic of Korea

†These authors contributed equally to this work.

*To whom correspondence should be addressed: mr0505@kbsi.re.kr and pkjhdn@kku.ac.kr

Table of contents

3. Supplementary Table

1. Supplementary Experimental Section

Characterization of RR-BA. The final product after the reaction was confirmed using reverse-phase HPLC (RP-HPLC; Agilent Technologies 1200 series, Santa Clara, CA, USA). All analyses were performed on an Eclipse Plus C18 reverse column (3.5 μm 4.6 × 150 mm; Agilent Technologies) by gradient elution with distilled water (90–10%) and acetonitrile (10–90%) containing 0.1% trifluoroacetic acid as the mobile phases at a flow rate of 1.0 mL/min. Detection was performed by ultraviolet-visible absorption at 224 nm. For one-dimensional ^{1}H and ^{13}C NMR analyses, we used a 500 MHz NMR spectrometer (JNM-ECZ500R/S1, JEOL, Tokyo, Japan). The samples were prepared in dimethylsulfoxide-d_6 at 2 and 10 mg/mL for ^{1}H and ^{13}C NMR measurements, respectively. The final volume of each sample was 600 μL. High performance liquid chromatography-mass spectrometry (HPLC-MS; Agilent Technologies 1260 infinity series) was utilized to identify RR-BA. Molecular weight of RR-BA was determined using atmospheric pressure ionization-electrospray techniques with a capillary voltage of 3000 V and a drying gas temperature of 350 °C in the positive scan mode. The calculated *m/z* value for $C_{38}H_{70}N_9O_5$ $[RR\text{-}BA + H]^+$ is 731.6, and the observed value is 731.5. The calculated *m/z* value for $C_{38}H_{71}N_9O_5$ $[RR\text{-}BA + 2H]^{2+}$ is 366.8, and the observed value is 366.9.

Cell viability test. The cytotoxicity of the synthesised molecules was evaluated using normal human fibroblasts (PromoCell, Heidelberg, Germany). The cells were cultured in Dulbecco's modified Eagle's medium containing 10% foetal bovine serum and 1% antibiotic-antimycotic solution. The cells were then seeded in a 96-well plate (SPL Life Sciences, Gyeonggi-do, Korea) at 1×10^4 cells/90 μL/well for the cell viability assay. The

solution containing the synthesised molecules (10 µL) was added to each well at different concentrations (final concentrations of 0.1–100 µM). After 24 h of incubation, cell viability was tested using an EZ-Cytox Cell Viability Assay Kit (Daeil Lab Service, Seoul, Korea). The UV absorbance was determined using a SPECTROstar Nano spectrophotometer (BMG Labtech, Ortenberg, Germany) at 450 nm. The cell viability (%) was calculated as the percentage of the UV absorbance value of the sample relative to that of the control (blank).

Expression and purification of ^{15}N-labelled Aβ42. Aβ42 was expressed and purified as previously described with some modifications.[1] Briefly, the DNA sequence encoding the human Aβ42 peptide was artificially constructed using codon optimisation for *Escherichia coli* with an extra Met residue at the N-terminus of the peptide. The DNA fragments were subcloned into the pAED4 vector,[2] and the resulting plasmid was transformed into the *E. coli* BL21 (DE3) pLysS strain (Novagen, Madison, WI, USA). The transformed cells were grown in Luria–Bertani (LB) medium containing ampicillin and chloramphenicol at 37 °C until reaching 3.5 McFarland turbidity, at which point the cells were harvested and transferred into an M9 minimal medium containing 2 g/L glucose and 1 g/L ^{15}N-labelled ammonium chloride, and 1 mM isopropyl β-$_D$-1-thiogalactopyranoside (IPTG) was added. The cells were cultured for 4 h at 37 °C. The peptide accumulated in the form of inclusion bodies in bacterial cells. The purified inclusion bodies were solubilised in 20 mM NaOH, and the peptide was further purified by repeated cycles of amyloid growth at low pH and monomerization in hexafluoroisopropanol (HFIP) combined with centrifugation. The monomerised and lyophilised peptides were dissolved in 20 mM NaOH at 4 °C and purified further using a

Source 15 RPC (Cytiva, Marlborough, MA, USA) HPLC column. The preparation ended with another HFIP monomerisation step.

Expression and purification of K18. To prepare non-labelled K18, the DNA sequence encoding K18 (residues 244–374) was cloned from full-length human tau and inserted into a pET vector. The 6× His-tagged K18 was expressed in *E. coli* BL21 (DE3) and purified using Ni-NTA (QIAGEN, Hilden, Germany) column chromatography as described previously.[3] Purified K18 was dissolved in 1× PBS (pH 7.4) and stored at -70 °C. For ^{15}N-labelled K18, the K18 gene was subcloned into the pET-15b vector, and the resulting plasmid was transformed into the *E. coli* Rosetta (DE3) strain. The transformed cells were grown in LB medium at 37 °C containing ampicillin until reaching an optical density at 600 nm of 0.8, at which point IPTG (0.5 mM) was added and the cells were incubated for an additional 4 h at 37 °C.

To culture the ^{13}C/^{15}N-labelled proteins, the *E. coli* cells were grown in M9 minimal medium supplemented with 2 g ^{13}C-glucose, 1 g ^{15}N-NH_4Cl, and 0.5 g/L ^{13}C/^{15}N-Celtone base powder. For ^{15}N-labelled proteins, 5 g glucose and 1 g ^{15}N-NH_4Cl (without Celtone powder) were added to the M9 minimal medium. All labelled materials were purchased from Cambridge Isotope Laboratories (Tewksbury, MA, USA). The cultured cells were harvested by centrifugation at 4,000 rpm for 30 min and stored at -70 °C. To purify the K18 protein, the cell pellet was resuspended in buffer (pH 7.0, 50 mM HEPES, 50 mM NaCl, 1.0 mM EDTA, 10 mM DTT, and 1.0 mM PMSF) and lysed by sonication. The cell lysate was incubated for 10 min in boiling water to precipitate most of the other proteins and then cooled on ice. After centrifugation (18,000 rpm) for 40 min at 4 °C, the supernatant was loaded onto a HiPrep-SP column (Cytiva). K18 protein was eluted using

a linear gradient of NaCl (0–1.0 M) at pH 7.0 (20 mM HEPES), concentrated using a Centricon (3 K MWCO, Millipore, Billerica, MA, USA), and applied to a Superdex-75 column (Cytiva) pre-equilibrated with a non-buffered solution containing only 50 mM NaCl at a pH value of ~6.0. Stock solutions of both non-labelled and ^{15}N-labelled K18 were subjected to buffer exchange with 20 mM sodium phosphate buffer (pH 7.5) using PD-10 columns (GE Healthcare Life Sciences, Little Chalfont, UK) before the experiments. The concentration of K18 was determined by measuring the absorbance at 280 nm (ε_{280} = 1,490 $M^{-1}\,cm^{-1}$)

Expression and purification of αSN. The gene encoding αSN (residues 1–140) was subcloned into the pET-41a vector, and the resulting plasmid was transformed into the *E. coli* Rosetta (DE3) strain. The transformed cells were grown in LB medium containing kanamycin at 37 °C until reaching an optical density at 600 nm of 0.8, after which IPTG (0.5 mM) was added and the cells were incubated for an additional 4 h at 37 °C. ^{15}N-Labelled proteins were cultured as described for K18. To purify αSN, the cell pellet was resuspended in buffer (pH 7.5, 50 mM HEPES, 1.0 mM EDTA, 2 mM DTT, and 1.0 mM PMSF) and disrupted by sonication. The cell lysate was incubated for 10 min in boiling water, and then cooled on ice. After centrifugation, the supernatant was loaded onto a HiPrep-Q column (Cytiva), and αSN was eluted using a linear gradient of NaCl (0–1.0 M) at pH 6.5 (20 mM sodium-phosphate). The eluted αSN protein was concentrated using a Centricon (5 K MWCO) and further purified via size exclusion column chromatography using a Superdex-75 pre-equilibrated with the same non-buffered solution. Stock solutions of αSN were subjected to buffer exchange with 20 mM sodium phosphate buffer (pH 7.4) using PD-10 columns (GE Healthcare) before the experiments. The αSN

concentration was determined by measuring the absorbance at 280 nm (ε_{280} = 5,960 M^{-1} cm^{-1}).

Preparation of monomeric Aβ42 solution. A stock solution of Aβ42 monomer was prepared as previously described with some modifications.[4] Briefly, lyophilised Aβ42 was dissolved in chilled NaOH solution (10 mM) at ~200 μM and sonicated in a cold-water bath for 15 s. To remove undissolved precipitates, the solutions were ultracentrifuged at 40,000 rpm at 4 °C for 1 h. The upper half of the supernatant was collected, and the concentration of Aβ42 was determined by measuring the absorbance at 280 nm (ε_{280} = 1,490 M^{-1} cm^{-1}).

Backbone resonance assignment of K18. To assign the backbone resonance of K18, $^{13}C/^{15}N$-labelled K18 was prepared in NMR buffer (pH 6.5, 50 mM MES, 50 mM NaCl, 1 mM DTT, and 5% D_2O), and then TROSY-based triple resonance NMR spectra (TROSY-HNCACB/HNcoCACB and TROSY-HNCO/HNcaCO) were recorded using a cryo-probed 800 MHz NMR spectrometer (Bruker, Billerica, MA, USA) at 10 °C. To resolve the sequential connectivity with similar chemical shifts, TROSY-HNcaNNH/TROSY-HncaNNH spectra were also recorded.[5] The NMR data were processed using the NMRpipe program.[6] The spectra were further analysed using the NMRFAM-Sparky program.[7]

DLS measurement. DLS measurements of RR-BA were performed on a Zetasizer NanoZS (Malvern Panalytical, Malvern, UK) at 25 °C. RR-BA (25 M) dissolved in 20 mM sodium phosphate buffer (pH 7.4) (50 μL) was loaded into a disposable microcuvette

(Model ZEN0040). The R_H was calculated using Zetasizer software (Malvern Panalytical, ver. 7.12).

AFM measurement. We applied 20 μL of the sample solution to a freshly cleaved mica plate, which was then incubated for 20–30 min. Each sample was gently rinsed twice with 20 μL of double deionised water. The remaining water was carefully removed using filter paper and compressed air. AFM measurements and analyses were conducted using an AFMPark NX10 (Park Systems Corp., Suwon, Korea).

Fluorescence dye-binding assay. The stocks of Nile red (1 mM) and curcumin (2 mM) were prepared in pure ethanol and DMSO, respectively. The working solutions for the two types of dye were freshly prepared by diluting their stocks in the desired buffer (20 mM sodium phosphate buffer (pH 7.5) and 100 mM NaCl). For fluorescence measurements, 33 μl of K18 amyloid fibril solutions generated with and without RR-BA was thoroughly mixed with 67 μl of dye working solutions. The final concentration of K18 monomers in amyloid fibril solutions was 10 μM. The final concentrations of Nile red and curcumin were 4 μM and 20 μM, respectively. The excitation wavelengths for Nile red and curcumin were 530 and 440 nm, respectively. A Cary Eclipse fluorescence spectrophotometer (Agilent. Technologies Inc., Santa Clara, CA, USA) was used to record the fluorescence emission spectra at 25 °C. All spectra were displayed after subtracting the background spectra from a solution without K18.

TEM measurement. TEM images were acquired using a JEM-1400 Plus TEM (JEOL Ltd., Tokyo, Japan) operated at 120 kV. Sample solutions containing K18 amyloid fibrils

(5 μl) were placed on collodion-coated copper grids (Nisshin EM Co., Tokyo, Japan) and allowed to adsorb for 1 min. Excess solution was removed using filter paper and subsequently, 5 μl of 2% (w/v) uranyl acetate solution was spotted onto the grids for sample staining. After 30 s, the remaining solution was blotted dry using filter paper

Biolayer interferometry assay. The binding affinity between RR-BA and αSN was determined by biolayer interferometry using a GatorPrime instrument (Gator96 system, Manufacturer, City, Country) at 35°C. Prior to the measurement, amine-reactive sensors (Gator probes, USA) were hydrated in distilled water for at least 10 min followed by 1x PBS buffer (pH 7.4) for 120 s. The hydrated sensors were then activated with NHS/EDC solution (10 mM/20 mM) for 400 s for amine coupling reaction, followed by loading αSN onto the sensors for 1,500 s at 2.5 μM. The sensors were quenched with 1 M ethanolamine solution (pH 8.5) for 300 s, and then equilibrated in 1x PBS buffer (pH 7.4) for 120 s. The association and dissociation of RR-BA was detected in 1x PBS buffer (pH 7.4) with 5 % DMSO for 300 s at an orbital shaking of 1,000 rpm. RR-BA was tested in the concentration range from 31.25 to 1000 μM. The steady-state response was analyzed using GatorOne Software.

Neuron-enriched mesencephalic cultures and αSN treatment. Neuron-enriched mesencephalic cultures were performed as previously described with some modification.[8] Briefly, C57BL/6N ventral mesencephalons were isolated from the embryonic day 13 (E13) fetal brain and dissected in Leibovitz's L-15 Medium (Welgene, Seoul, Korea). The dissected segments were incubated in 0.01 % trypsin solution diluted in Ca^{2+}-, Mg^{2+}-free HBSS (Life Technologies, Rockville, MD, USA) at 37 ^{o}C for 10 mins,

and incubated at 37 ^{o}C in 100 μg/ml DNase I diluted in DMEM medium (Life Technologies) for additional 5 mins. The tissues were mechanically triturated in DMEM medium supplemented with 10 % FBS and 100 U/ml penicillin/streptomycin (P/S). The dissociated cells were plated on 8-well slides pre-coated with 100 μg/ml poly-D-lysine and 40 μg/ml laminin at a density of 7 x 10^5 cells/ml (300 μl/well). The cells were incubated in a humidified incubator at 37 ^{o}C, 5 % CO_2 for 24 h and replaced with serum-free Ham's nutrient mixture (F12-DMEM, Life Technologies) supplemented with 1 % ITS (insulin, transferrin, selenium) and P/S. At DIV 4, the neurons were treated with 30 μM of αSN which was incubated with and without RR-BA for 12 h. After 48 h, neurons were processed for immunocytochemical analysis.

Immunocytochemistry and image analysis. Immunocytochemical staining was performed as previously described with some modification.[8] Briefly, neurons were fixed with 4 % paraformaldehyde at room temperature for 30 mins. The cells were rinsed with PBS, permeabilized using PBS containing 0.2 % triton X-100 and 1 % BSA at room temperature for 5 mins, and then incubated with anti-tyrosine hydroxylase antibody (TH, Merck) diluted in PBS containing 0.5 % BSA at 4 ^{o}C for overnight to visualize dopaminergic neurons. The cells were then rinsed with PBS containing 0.5 % BSA and incubated with alexa fluor 488 affinipure donkey anti-rabbit IgG (H+L) (Jackson immunoresearch, PA, USA). After 1 h, the cells were rinsed with 0.1 M phosphate buffer and mounted with VECTASHIELD Antifade Mounting Medium with DAPI (vector laboratories, CA, USA). The stained cells were captured under a slide scanner (3DHISTECH, Budapest, Hungary). TH^+ cell number and neurite outgrowth were analyzed using Metamoph software (Moecular devices, CA, USA).

2. Supplementary Figures

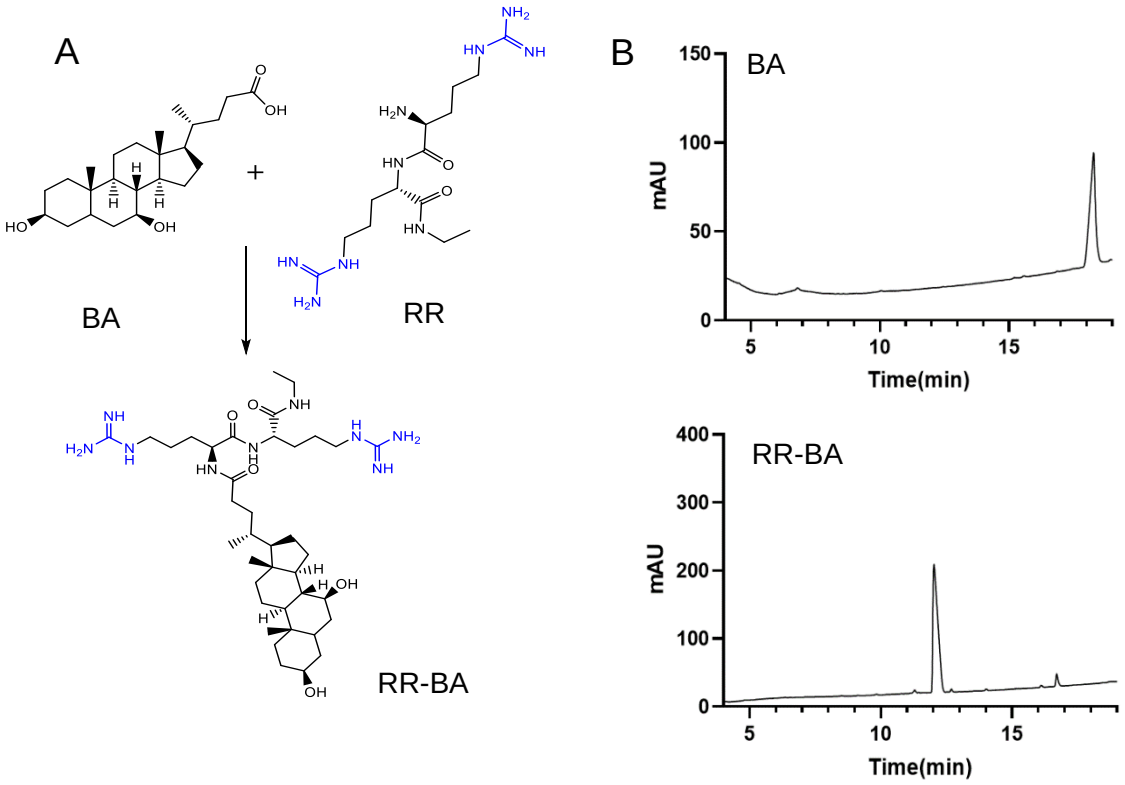

Figure S1. Synthesis and purification of RR-BA. (**A**) Synthetic scheme of RR-BA with BA and RR. BA and RR were conjugated via the EDC/NHS reaction to prepare RR-BA. (**B**) Synthesised product (RR-BA) was purified and confirmed using reversed-phase HPLC (lower panel) and compared with BA to determine the sample purity (upper panel). Hydrophilic RR was not detectable in the profile of RR-BA, indicating high purity.

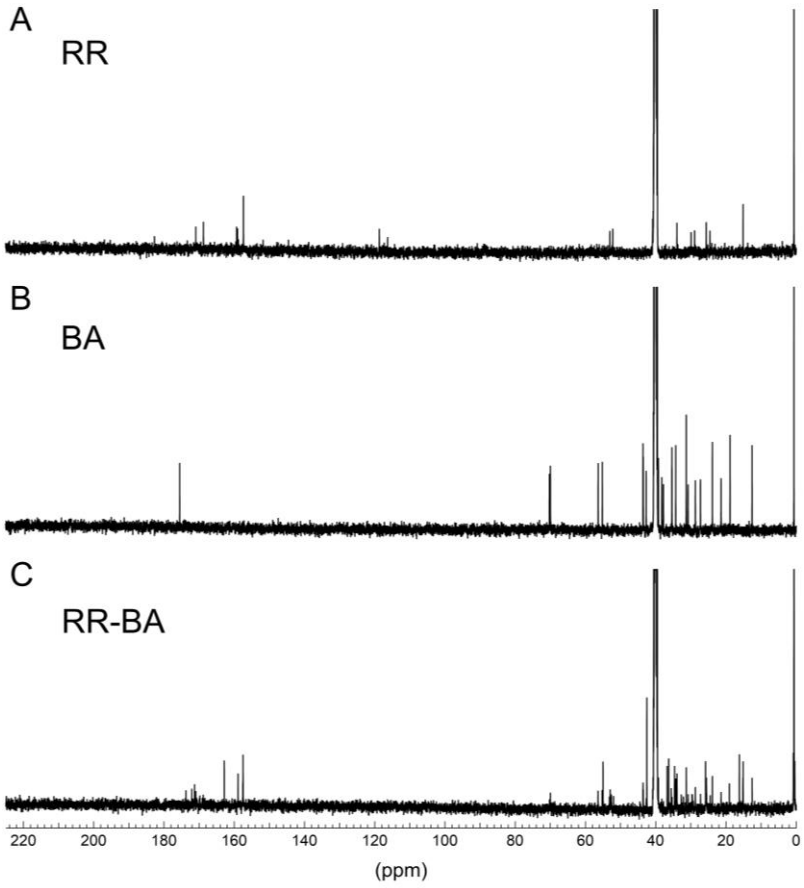

Figure S2. ^{13}C NMR characterization of RR-BA. (**A**-**C**) ^{13}C NMR spectra of positively charged RR (**A**), hydrophobic BA (**B**), and synthesised amphiphilic conjugate (RR-BA) (**C**) in DMSO-d_6.

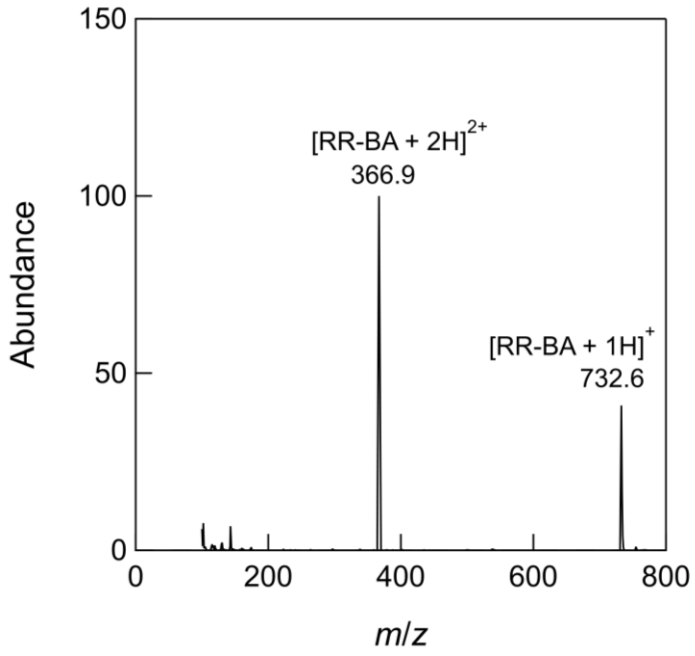

Figure S3. Mass spectrum of RR-BA. HPLC-MS chromatogram of synthesised amphiphilic conjugate (RR-BA) in positive mode.

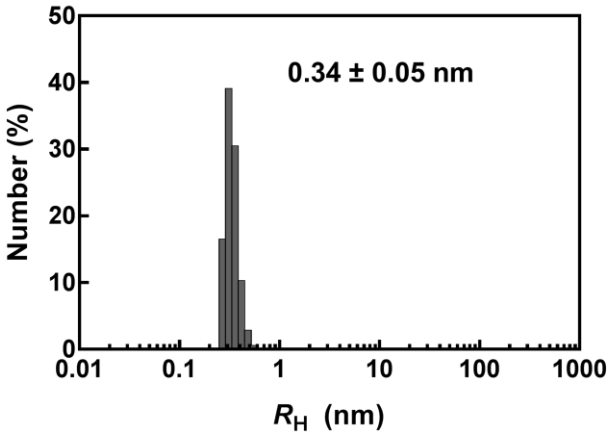

Figure S4. Measurement of R_H of RR-BA using DLS. The distribution of the R_H of RR-BA analysed using DLS. The average and error of R_H obtained from the triplicate measurements is shown.

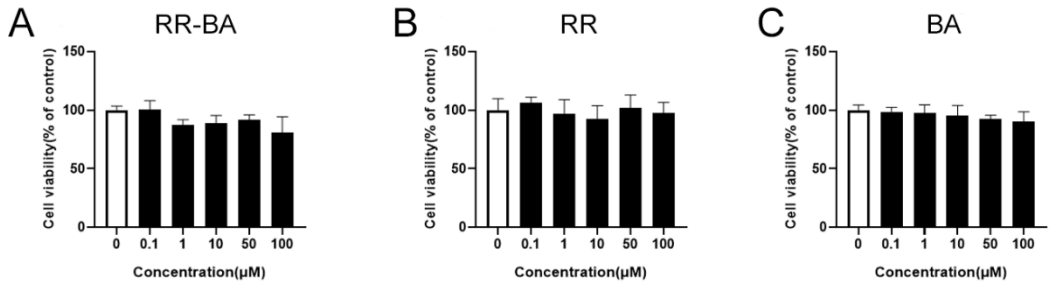

Figure S5. Cytotoxicity of synthesised molecules. (**A**–**C**) Normal human fibroblasts were incubated with RR-BA (**A**), RR (**B**), and BA (**C**) for 24 h, and cell viability was determined using a UV/Vis spectrophotometer. Error bars represent the standard deviation.

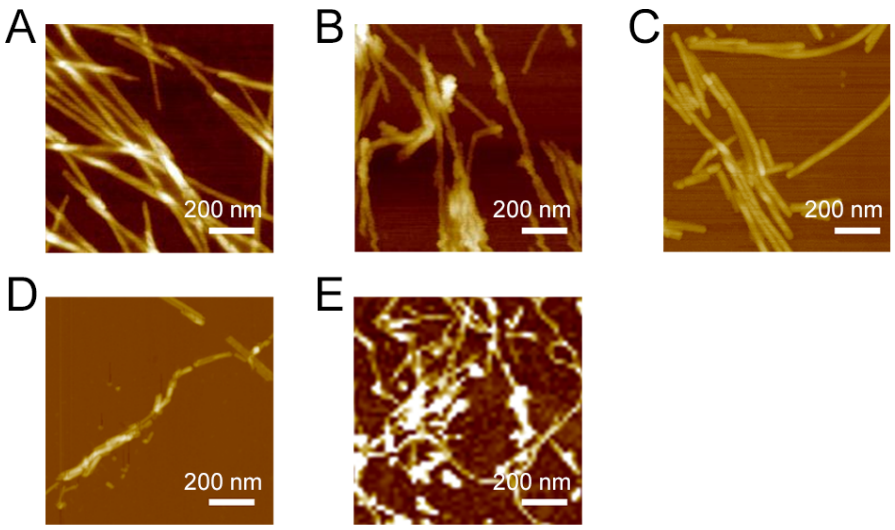

Figure S6. Morphological characterization of protein aggregates formed after ThT fluorescence assay. (**A**–**C**) AFM images of αSN amyloid fibrils in the absence (**A**) and presence of 5 molar equivalents of RR-BA (**B**) or RR (**C**). (**D** and **E**)AFM images of K18 (**D**) and Aβ42 (**E**) amyloid fibrils formed without RR-BA and RR. Scale bars represent 200 nm.

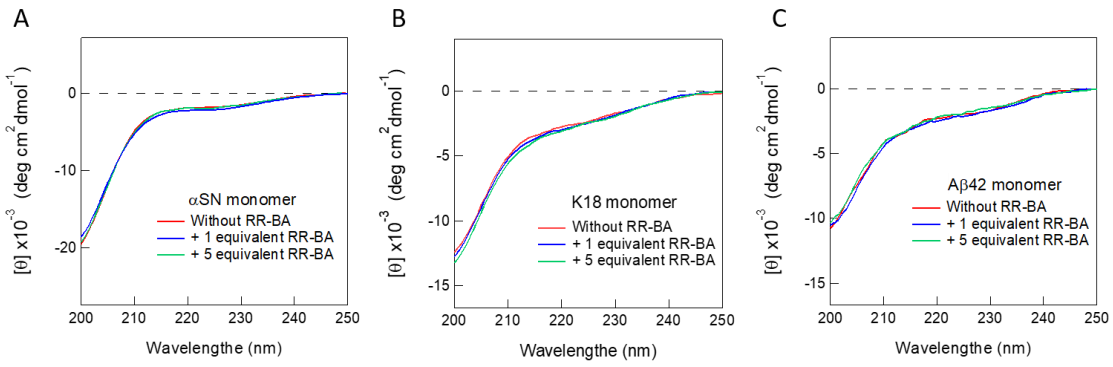

Figure S7. Influences of RR-BA on monomeric structures of three types of amyloidogenic proteins. (**A**-**C**) Far-UV CD spectra of αSN (**A**), K18 (**B**), and Aβ42 (**C**) were obtained in the absence and presence of RR-BA. The CD spectra acquired at different concentrations of RR-BA are displayed in distinct colours: red (without RR-BA), blue (1 molar equivalent of RR-BA), and green (5 molar equivalents of RR-BA).

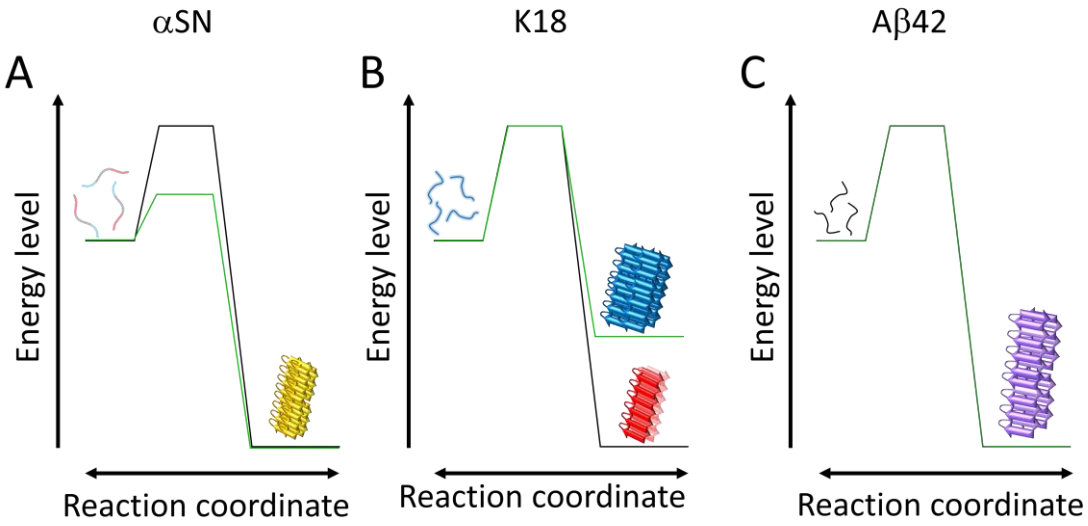

Figure S8. Conceptual energy landscapes of amyloid formation of αSN, K18, and Aβ42. (**A**–**C**) Relative energy levels between monomers and amyloid fibrils for thermodynamics and activation energy barriers controlling kinetics of amyloid formation are represented for αSN (**A**), K18 (**B**), and Aβ42 (**C**). Black and green lines indicate the conceptual energy landscape in the absence and presence of RR-BA, respectively. Cartoons of disordered monomers (left) and amyloid fibrils (right) are shown in each energy landscape. Distinct types of monomers and amyloid fibrils are shown in different colours. In B, the different amyloid fibrils of K18 in the higher (blue) and lower (red) energy levels have the same activation energy.

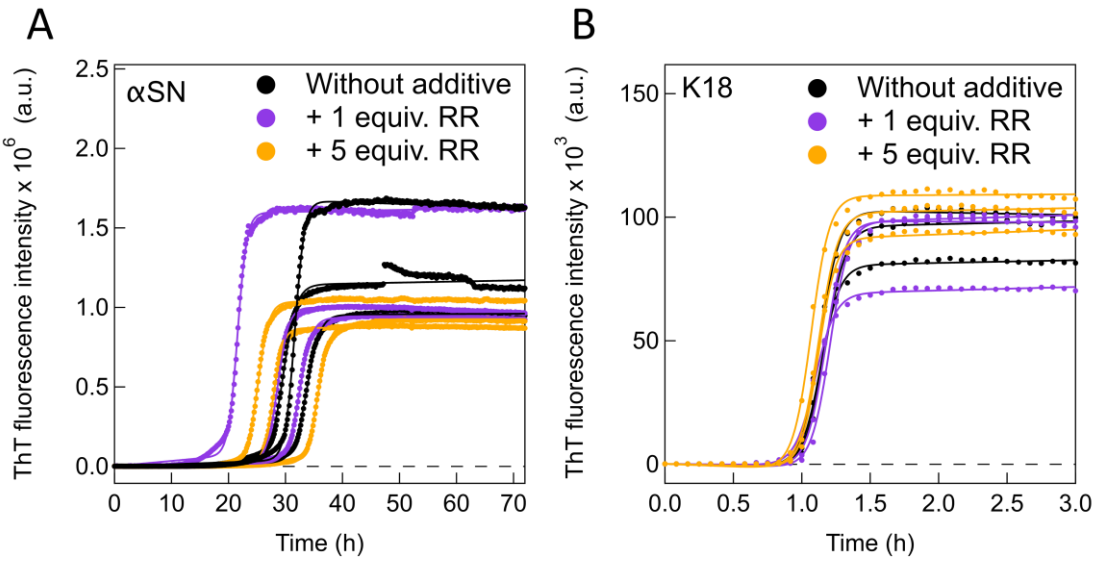

Figure S9. ThT-based real-time monitoring of amyloid formation of αSN and K18 in the presence of RR. (**A** and **B**) Amyloid formation of αSN (**A**) and K18 (**B**) with and without 1 or 5 molar equivalents of RR was traced using ThT fluorescence assay. Solid lines indicate the fit curves.

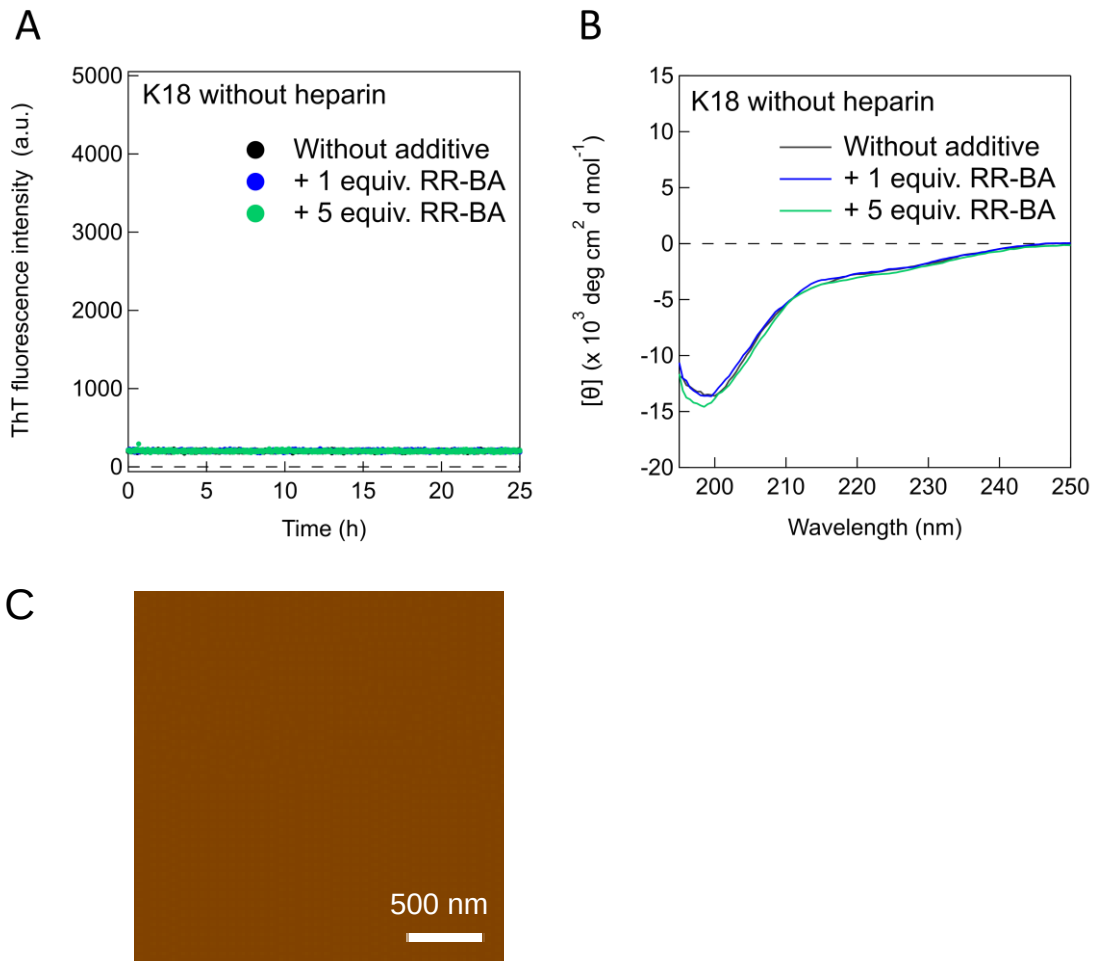

Figure S10. Monitoring of K18 amyloid fibrillation without heparin. (**A** and **B**) Aggregation of K18 in the absence of heparin examined using ThT fluorescence assay (**A**) and CD spectroscopy (**B**)**.** ThT intensity of K18 in the absence (black) and presence of 1 (blue) or 5 (green) molar equivalents of RR-BA plotted as a function of the incubation time. The post-incubation far-UV CD spectra of K18 samples were recorded. (**C**) AFM micrograph of K18 sample solution incubated without heparin and BA. Scale bar represents 500 nm.

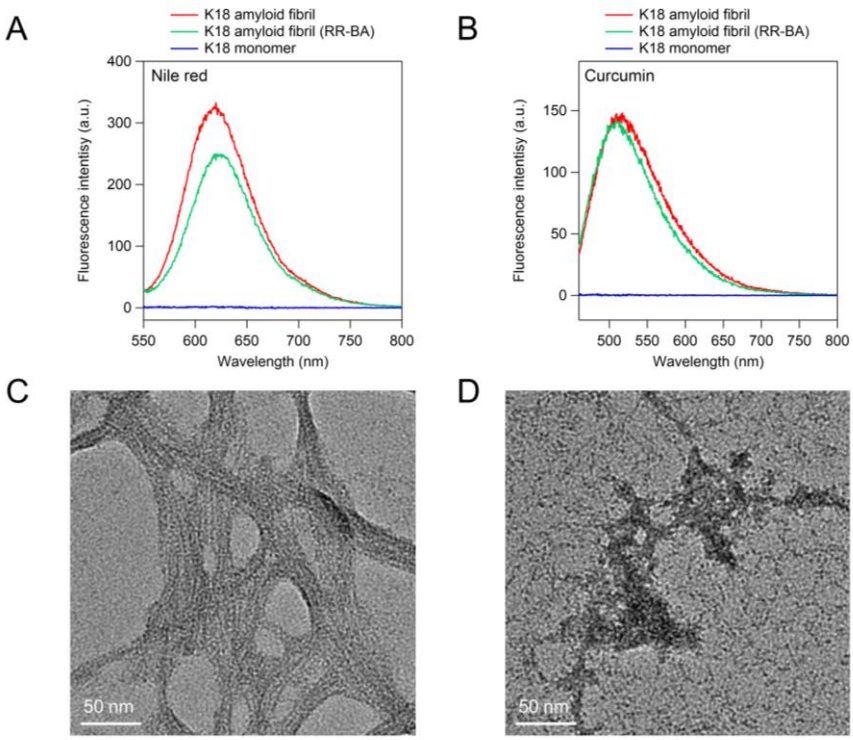

Figure S11. RR-BA-induced polymorphic amyloid generation of K18. (**A** and **B**) The fluorescence spectra of Nile red (**A**) and curcumin (**B**) in the presence of K18 amyloid fibrils grown with and without RR-BA. The fluorescence spectra of Nile red and curcumin in the presence of K18 monomer are also shown for comparison. (**C** and **D**) TEM micrographs of K18 amyloid fibrils grown in the absence (**C**) and presence RR-BA (**D**) (scale bar = 50 nm).

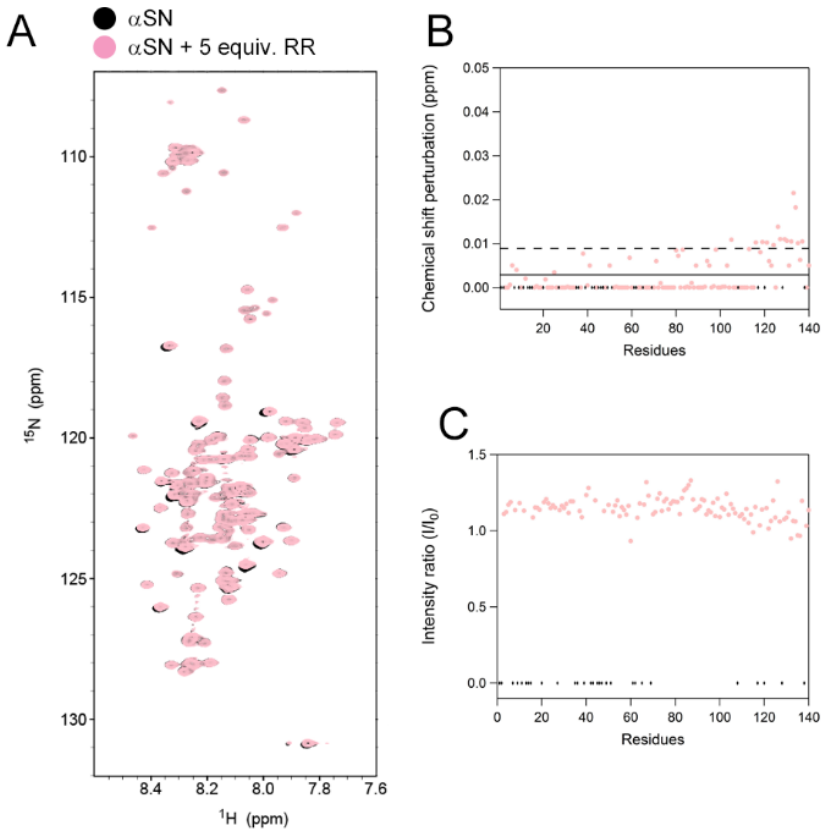

Figure S12. Molecular interactions between RR and αSN probed using NMR. (**A**) 2D ^{1}H-^{15}N HSQC NMR spectra of ^{15}N-labelled αSN monomers in the absence (black) and presence (pink) of 5 molar equivalents of RR. (**B** and **C**) CSPs (**B**) and peak intensity ratio (**C**) of αSN upon addition of 5 molar equivalents of RR-BA. Two horizontal lines represent the average chemical shift (solid line) plus one standard deviation (dashed line). The amino acid residues that could not be analysed because of overlapping or unassigned chemical shifts are indicated by black diamonds.

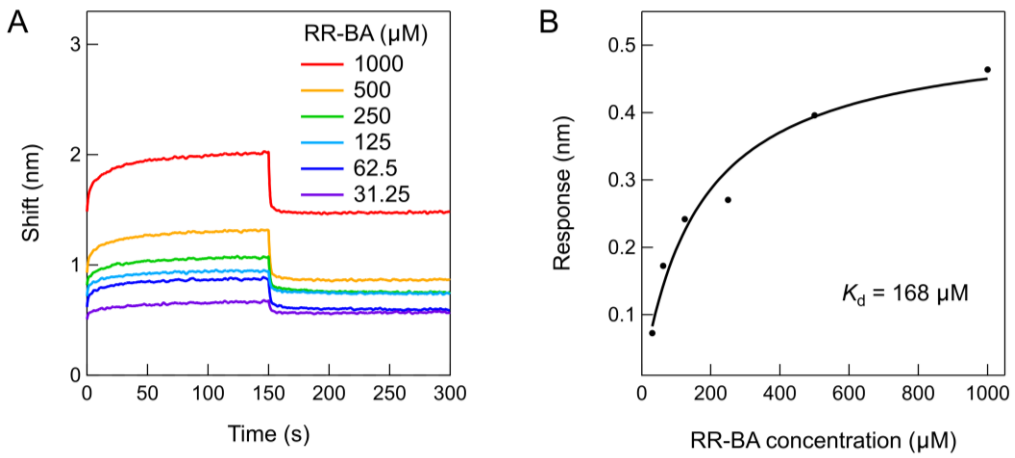

Figure S13. BLI analysis of the interaction between RR-BA and αSN. (**A**) BLI sensorgram of RR-BA binding to αSN. (**B**) BLI steady-state analysis of the binding affinity of RR-BA to αSN. K_d value obtained from the fitting analysis is displayed.

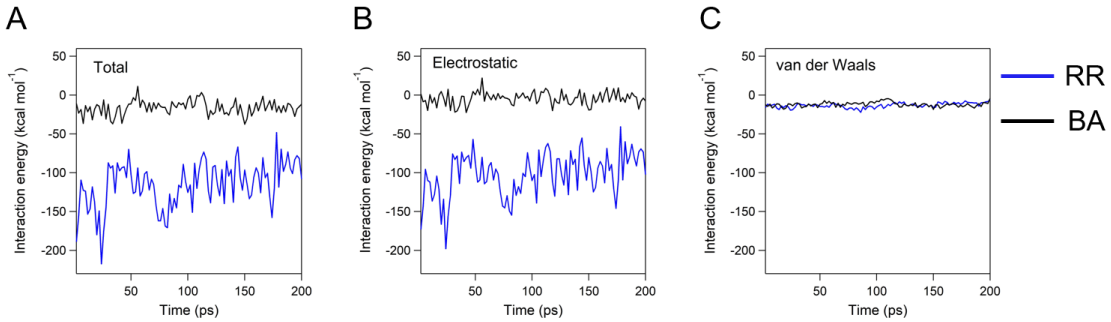

Figure S14. Time evolution of molecular interaction energies between RR-BA and αSN. (**A**-**C**) The total interaction energy (**A**), electrostatic interaction energy (**B**), and van der Waals interaction energy (**C**) for the binding of RR (blue) or BA (black) to αSN were plotted as a function of time.

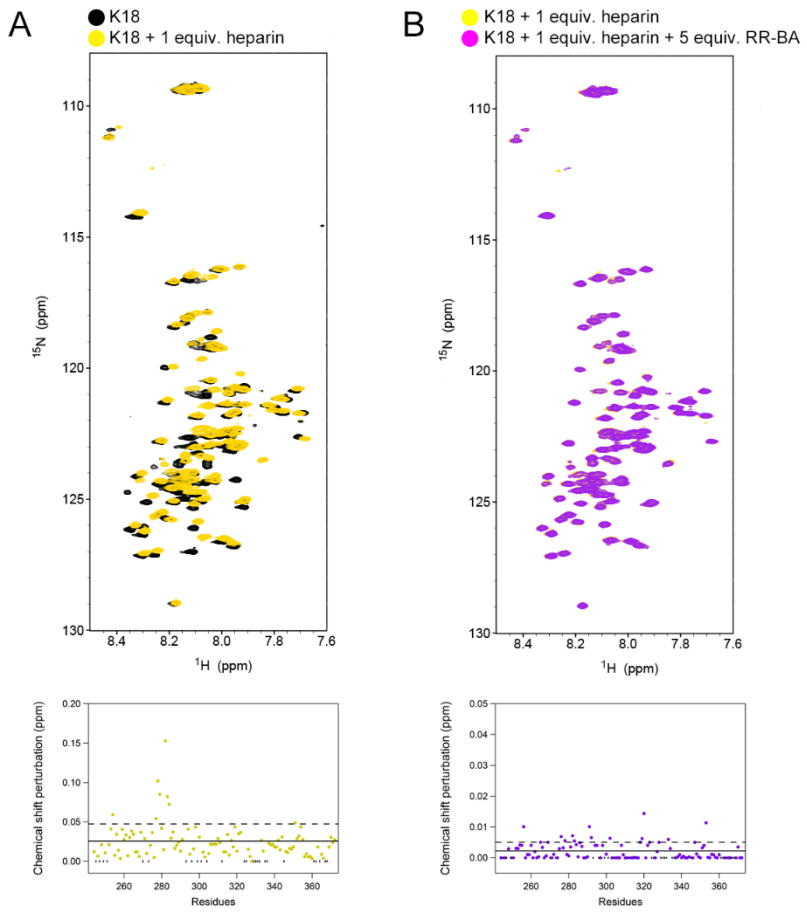

Figure S15. NMR investigation of the intermolecular interaction between RR-BA and K18 in the presence of heparin. (**A**) 2D ^{1}H-^{15}N BEST-TROSY spectra of ^{15}N-labelled K18 monomers (50 μM) alone (black) and after the addition of 50 μM heparin (yellow) (upper panel). CSPs of K18 following the addition of 50 μM heparin (lower panel). (**B**) 2D NMR spectra of 50 μM K18 with 50 μM heparin in the absence (yellow) and presence of 250 μM RR-BA (purple) (upper panel). CSPs of K18 with 50 μM heparin following the addition of 250 μM RR-BA (lower panel). Two horizontal lines indicate the average chemical shift (solid line) plus one standard deviation (dashed line). The amino acid residues that could not be analysed because of overlapping or unassigned chemical shifts are indicated by black diamonds.

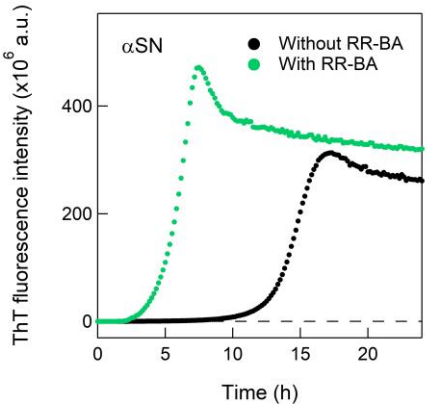

Figure. S16. ThT-based real-time monitoring of αSN amyloid formation at 300 μM. Amyloid formation of αSN at 300 μM with and without 5 molar equivalents of RR-BA was traced using ThT fluorescence assay.

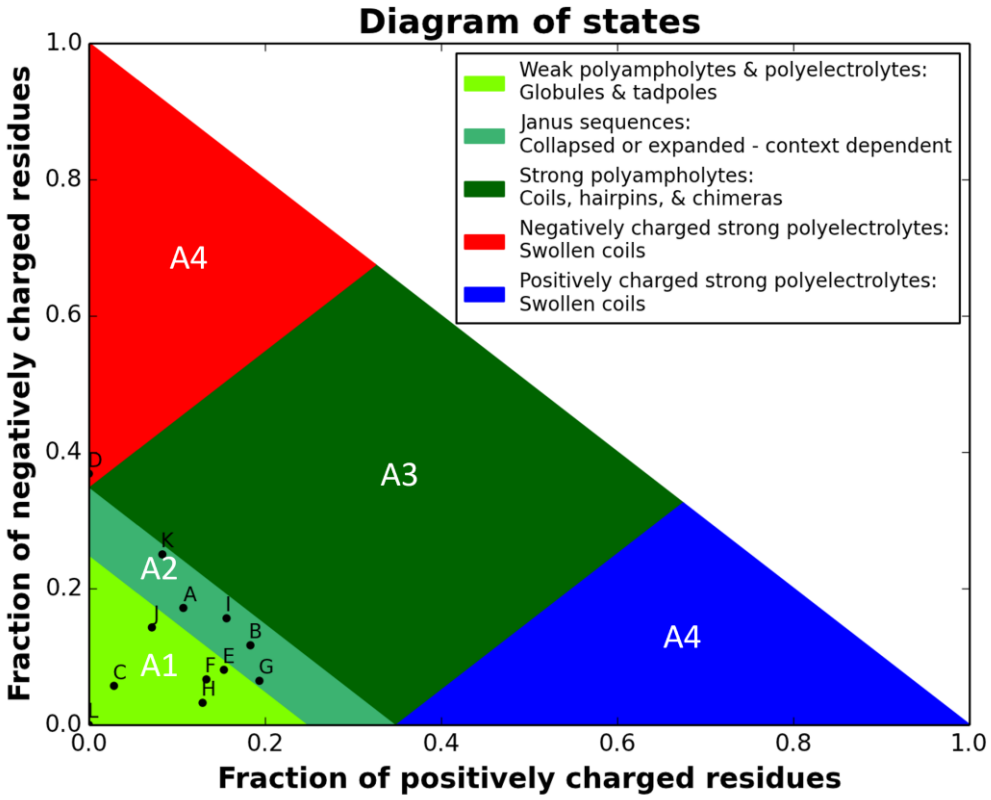

Figure S17. Das-Pappu diagram of αSN, K18, and Aβ42. Location of each protein and its fragment in the Das-Pappu diagram: full-length αSN (A), αSN N-terminal region (residues 1–60) (B), αSN NAC region (residues 61–95) (C), αSN C-terminal region (residues 103–140) (D), full-length K18 (E), K18 R1 region (residues 244–273) (F), K18 R2 region (residues 274–304) (G), K18 R3 region (residues 305–335) (H), K18 R4 region (residues 336–367) (I), full-length Aβ42 (J), Aβ42 N-terminal region (residues 1–24) (K), and Aβ42 C-terminal region (residues 29–42) (L). The x- and y-axes represent the fractions of positively and negatively charged residues, respectively. The diagram is divided into four areas, A1–A4, according to the fraction of charged residues and net charge per residue.

3. Supplementary Table

	H (%)	P (%)	AP (%)	T (%)	O (%)
αSN only	0.0	0.0	28.1	23.3	48.6
αSN + 1 molar equivalent of RR-BA	0.0	0.0	26.1	23.3	50.6
αSN + 5 molar equivalents of RR-BA	0.0	0.0	27.6	23.2	49.1

Table S1. Contents of the secondary structure of monomeric αSN in the presence and absence of RR-BA. The secondary structure contents of αSN monomers were analyzed in the absence and presence of 1 or 5 molar equivalents of RR-BA using the BeStSel algorithm.[9] The following abbreviations were used: H, helix; P, parallel β-strand; AP, antiparallel β-strand; T, Turn; O, Others. Others mainly represent disordered structures.

4. Supplementary References

1. T. Ikenoue, Y. H. Lee, J. Kardos, M. Saiki, H. Yagi, Y. Kawata and Y. Goto, *Angew. Chem. Int. Ed. Engl.*, 2014, **53**, 7799-7804.
2. C. J. McKnight, D. S. Doering, P. T. Matsudaira and P. S. Kim, *J. Mol. Biol.*, 1996, **260**, 126-134.
3. D. Kim, S. Lim, M. M. Haque, N. Ryoo, H. S. Hong, H. Rhim, D. E. Lee, Y. T. Chang, J. S. Lee, E. Cheong, D. J. Kim and Y. K. Kim, *Sci. Rep.*, 2015, **5**, 15231.
4. J. Roche, Y. Shen, J. H. Lee, J. Ying and A. Bax, *Biochemistry*, 2016, **55**, 762-775.
5. R. Weisemann, H. Ruterjans and W. Bermel, *J. Biomol. NMR*, 1993, **3**, 113-120.
6. F. Delaglio, S. Grzesiek, G. W. Vuister, G. Zhu, J. Pfeifer and A. Bax, *J. Biomol. NMR*, 1995, **6**, 277-293.
7. W. Lee, M. Tonelli and J. L. Markley, *Bioinformatics*, 2015, **31**, 1325-1327.
8. S. Bhurtel, E. Bok, N. Katila, J. Kim and D. Y. Choi, *Biochem Pharmacol*, 2021, **192**, 114719.
9. A. Micsonai, F. Wien, L. Kernya, Y. H. Lee, Y. Goto, M. Refregiers and J. Kardos, *Proc. Natl. Acad. Sci. U. S. A.*, 2015, **112**, E3095-3103.